ASIAN JOURNAL OF CIVIL ENGINEERING (BHRC) VOL. 18, NO. 2(2017)
PAGES 207-234

LARGE DEFLECTION OF ARBITRARY THIN PLATES USING SUPERPARAMETRIC FINITE ELEMENT

S. Panda and M. Barik*
Department of Civil Engineering, National Institute of Technology, Rourkela, Odisha 769008, India

Received: 15 March 2016; **Accepted:** 26 August 2016

ABSTRACT

Different arbitrary shapes of plates are used in civil, marine and aerospace engineering. They may undergo large deflections due to large transverse loads and hence, the nonlinear analysis must be carried out on the structures. In view of the above an elegant finite element formulation is developed for analyzing the geometrically nonlinear static behavior of arbitrary shaped thin plates using superparametric element. This element is capable of accommodating different geometries just like isoparametric element. The efficacy of the element is shown by presenting different numerical examples.

Keywords: Finite element analysis; large deflection; nonlinear plate theory; arbitrary thin plates; superparametric element.

1. INTRODUCTION

The arbitrary shaped plates especially in civil, marine and aerospace engineering may undergo large deflections under transverse loads. The value of lateral displacement obtained by the large deflection analysis will be significantly less than that obtained with linear analysis shown in Fig.1 as the structure becomes stiffer. Hence the additional effects due to large deflection must be considered in the analysis.

The geometrically nonlinear analyses of the plates have been attempted by many researchers in the past. Levy [1] analytically solved clamped square plate using differential equation of Timoshenko, Von-Karman's equation and Fourier series. The finite element analysis of the same plate is done by Bogner et al. [2] using a conforming rectangular element with sixteen degrees of freedom. Schmidt [3] used perturbation method and Rushton [4] used finite difference dynamic relaxation solution to solve clamped circular plate and simply supported square plate respectively. The performance of linear, serendipity, Lagrangian and Heterosis elements is presented by Pica et al. [5] for various shapes of plates

*E-mail address of the corresponding author: manoranjanbarik@yahoo.co.in (M. Barik)

using a Mindlin formulation. As usual, they faced the latent problem of isoparametric formulation like shear locking and the spurious energy modes. Though they have tried to alleviate the above problems by reduced and selective integration, the behavior of the elements were inconsistent depending on whether a boundary is straight or curved. Cheung and Dashan [6] considered finite strip method to study arbitrary shaped thin plates. Annular sector plate is analyzed by Turvey and Salehi [7] using a dynamic relaxation finite difference procedure. Singh and Elaghabash [8] proposed a numerical method (Ritz type) for the linear and geometrically non-linear static analysis of rhombic plates. The plate geometry is defined by a quadrangular boundary with four straight edges and the natural coordinates in conjunction with the Cartesian coordinates are used to map the geometry. Spline finite strip method is used by Sheikh and Mukhopadhyay [9] to analyze plates of different geometries. They have discretized mapped domain into a number of strips using cubic serendipity function and used two different displacement interpolation function in longitudinal and the other direction. A mathematical model is formulated by Shahidi et al. [10] based on elastic Cosserat theory for analysis of arbitrary quadrilateral plates. Das et al. [11] studied the isotropic skew plates under uniformly distributed load using variational principle. The effect of transverse shear was included in a shell element for geometric nonlinear analysis by Wankhade [12]. His work provided brief study of skew plates with variable parameters.

In the present analysis, the geometrically nonlinear static behavior of arbitrary shaped thin plates is studied using superparametric element. The cubic serendipity function is used to represents the arbitrary geometry of the plate. An ACM plate ([13], [14]) bending element along with the in-plane deformations is considered for the displacement function. This element is capable of accommodating different geometries just like isoparametric element. As this element considers only thin plates and hence, does not consider the shear deformation, thus eliminating the shear locking problem and generation of spurious mechanisms. In the formulation the arbitrary planform of the whole plate is mapped into a square domain and the nonlinear formulation uses Von-Karman's nonlinear equation in the total Lagrangian coordinate system using [N]-notation. The nonlinear governing equations are solved by Newton Raphson iterative method. The deflections and stresses at critical points of the plates of different shapes are compared with the published results. The new results are compared with the SAP 2000 results wherever possible.

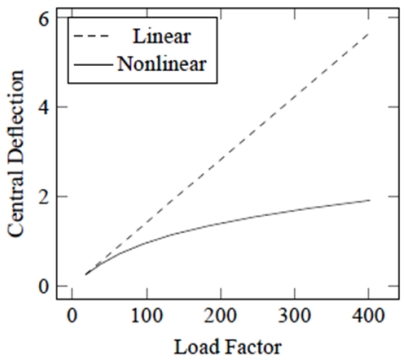

Figure 1. Small and large deflection theory

2. MAPPING OF THE PLATE

The arbitrary shape of the plate is mapped [15] approximately into a $[-1,+1]$ region in the $s-t$ plane as shown in Fig.2 with the help of the cubic serendipity shape function [16].

$$x = \sum_{i=1}^{12} N_i(s,t)x_i \tag{1}$$

$$y = \sum_{i=1}^{12} N_i(s,t)y_i \tag{2}$$

where (x_i, y_i) are the co-ordinates of the i-th boundary node of the plate and N_i is the corresponding cubic serendipity shape function. The mapped square plate is now discretized into a number of elements and each element is being mapped with the same cubic serendipity shape function to a natural coordinate element of domain $[-1,+1]$ in $\xi-\eta$ plane as shown in Fig. 3.

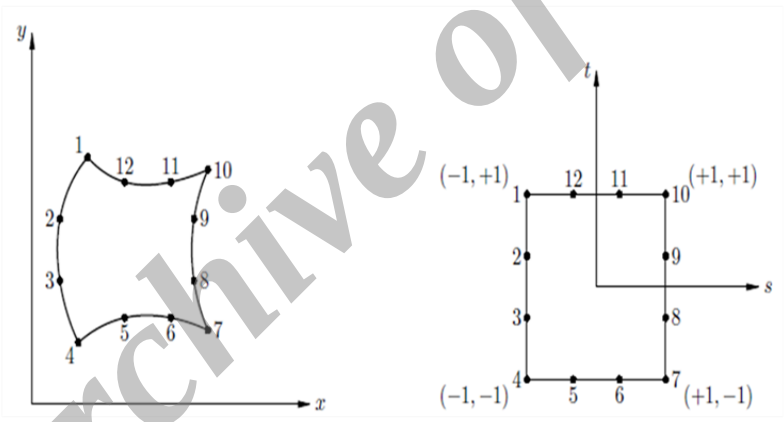

Figure 2. Mapping of arbitrary geometry into a square domain in $s-t$ plane

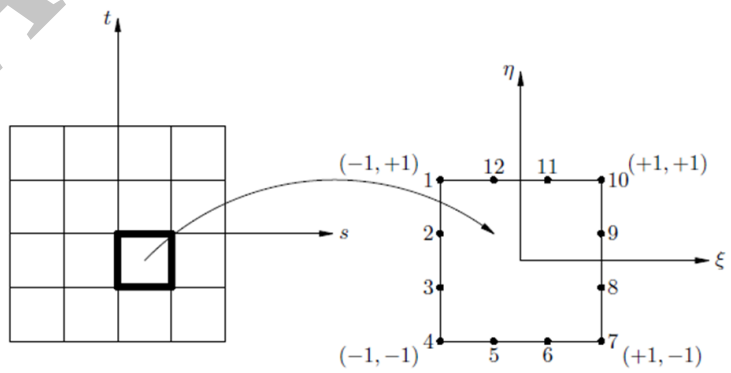

Figure 3. Mapping of element into a square domain in $\xi-\eta$ plane

From the mapping we have,

$$\begin{Bmatrix} \frac{\partial w}{\partial x} \\ \frac{\partial w}{\partial y} \end{Bmatrix} = [J]^{-1} \begin{Bmatrix} \frac{\partial w}{\partial \xi} \\ \frac{\partial w}{\partial \eta} \end{Bmatrix} \tag{3}$$

$$\text{where, } [J] = \begin{Bmatrix} \frac{\partial x}{\partial \xi} & \frac{\partial y}{\partial \xi} \\ \frac{\partial x}{\partial \eta} & \frac{\partial y}{\partial \eta} \end{Bmatrix} \tag{4}$$

3. DISPLACEMENT INTERPOLATION FUNCTION

For the proposed element, the four noded rectangular ACM plate bending element with five degrees of freedom $(u, v, w, \frac{\partial w}{\partial x}, \frac{\partial w}{\partial y})$ at each node is considered. The interpolation functions for the in-plane and bending are the usual ones presented in detail in [17].

4. STRESS-STRAIN RELATIONSHIP

The generalized stress-strain relation is given by

$$\{\sigma\} = [D]\{\varepsilon\} \tag{5}$$

where, $\{\sigma\}$ is the stress resultant given by

$$\{\sigma\} = \begin{Bmatrix} \{\sigma^p\} \\ \{\sigma^b\} \end{Bmatrix} = \begin{Bmatrix} N_x \\ N_y \\ N_{xy} \\ M_x \\ M_y \\ M \end{Bmatrix}_{xy}, \tag{6}$$

and $[D]$ is the rigidity matrix given by

$$[D]=\begin{bmatrix}[D^p] & [0]\\ [0] & [D^b]\end{bmatrix} \tag{7}$$

where, $[D^p]=\dfrac{Eh}{1-\nu^2}\begin{bmatrix}1 & \nu & 0\\ \nu & 1 & 0\\ 0 & 0 & \dfrac{1-\nu}{2}\end{bmatrix}$

$$[D^b]=\frac{Eh^3}{12(1-\nu^2)}\begin{bmatrix}1 & \nu & 0\\ \nu & 1 & 0\\ 0 & 0 & \dfrac{1-\nu}{2}\end{bmatrix}$$

The superscripts p and b used in the equations are for the inplane and bending part respectively. Taking the mid-plane of the plate as the reference plane for the analysis, strain matrix is given by

$$\{\varepsilon\}=\begin{bmatrix}\{\varepsilon^p\}_L\\ \{\varepsilon^b\}_L\end{bmatrix}+\begin{bmatrix}\{\varepsilon^p\}_{NL}\\ \{\varepsilon^b\}_{NL}\end{bmatrix}$$

$$=\begin{pmatrix}\dfrac{\partial u}{\partial x}\\ \dfrac{\partial v}{\partial y}\\ \dfrac{\partial u}{\partial y}+\dfrac{\partial v}{\partial x}\\ ---\\ -\dfrac{\partial^2 w}{\partial x^2}\\ -\dfrac{\partial^2 w}{\partial y^2}\\ -2\dfrac{\partial^2 w}{\partial x\partial y}\end{pmatrix}+\begin{pmatrix}\dfrac{1}{2}\left(\dfrac{\partial w}{\partial x}\right)^2\\ \dfrac{1}{2}\left(\dfrac{\partial w}{\partial y}\right)^2\\ \left(\dfrac{\partial w}{\partial x}\right)\left(\dfrac{\partial w}{\partial y}\right)\\ ---\\ 0\\ 0\\ 0\end{pmatrix} \tag{8}$$

5. STRAIN DISPLACEMENT RELATIONSHIP

The strain displacement relation is given by

$$\{\varepsilon^p\}_L = \{B^p\}_L\{\delta\} \tag{9}$$

$$\{\varepsilon^p\}_{NL} = \{B^p\}_{NL}\{\delta\} \tag{10}$$

$$\{\varepsilon^b\}_L = \{B^b\}_L\{\delta\} \tag{11}$$

The inplane linear strain is given by

$$\begin{Bmatrix} \frac{\partial u}{\partial y} \\ \frac{\partial v}{\partial x} \\ \frac{\partial u}{\partial y}+\frac{\partial v}{\partial x} \end{Bmatrix} = \begin{bmatrix} \frac{\partial \xi}{\partial x} & \frac{\partial \eta}{\partial x} & 0 & 0 \\ 0 & 0 & \frac{\partial \xi}{\partial y} & \frac{\partial \eta}{\partial y} \\ \frac{\partial \xi}{\partial y} & \frac{\partial \eta}{\partial y} & \frac{\partial \xi}{\partial x} & \frac{\partial \eta}{\partial x} \end{bmatrix} \begin{Bmatrix} \frac{\partial u}{\partial \xi} \\ \frac{\partial u}{\partial \eta} \\ \frac{\partial v}{\partial \xi} \\ \frac{\partial v}{\partial \eta} \end{Bmatrix} \tag{12}$$

$$\{\varepsilon^p\}_L = [T_L^p]\{\varepsilon(\xi,\eta)\} \tag{13}$$

$$\{B^p\}_L = [T_L^p]\begin{Bmatrix} \frac{\partial N_u}{\partial \xi} \\ \frac{\partial N_u}{\partial \eta} \\ \frac{\partial N_v}{\partial \xi} \\ \frac{\partial N_v}{\partial \eta} \end{Bmatrix} \tag{14}$$

The linear strain due to bending [15] action is given by

$$\begin{Bmatrix} -\frac{\partial^2 w}{\partial x^2} \\ -\frac{\partial^2 w}{\partial y^2} \\ -2\frac{\partial^2 w}{\partial x \partial y} \end{Bmatrix} = \begin{bmatrix} T^{b1} & T^{b2} \end{bmatrix} \begin{Bmatrix} \frac{\partial w}{\partial \xi} \\ \frac{\partial w}{\partial \eta} \\ \frac{\partial w}{\partial \eta} \\ \frac{\partial^2 w}{\partial \xi^2} \\ \frac{\partial^2 w}{\partial \eta^2} \\ \frac{\partial^2 w}{\partial \xi \partial \eta} \end{Bmatrix} \tag{15}$$

$$\{B^b\}_L = \begin{bmatrix} T^{b1} & T^{b2} \end{bmatrix} \begin{Bmatrix} \frac{\partial N_w}{\partial \xi} \\ \frac{\partial N_w}{\partial \eta} \\ \frac{\partial^2 N_w}{\partial \xi^2} \\ \frac{\partial^2 N_w}{\partial \eta^2} \\ \frac{\partial^2 N_w}{\partial \xi \partial \eta} \end{Bmatrix} \tag{16}$$

where, $[T^{b1}] = [J2]^{-1}[J1][J]^{-1}$

$[T^{b2}] = [J2]^{-1}$

$$[J1] = \begin{bmatrix} \frac{\partial^2 x}{\partial \xi^2} & \frac{\partial^2 y}{\partial \xi^2} \\ \frac{\partial^2 x}{\partial \eta^2} & \frac{\partial^2 y}{\partial \eta^2} \\ \frac{\partial^2 x}{\partial \xi \partial \eta} & \frac{\partial^2 y}{\partial \xi \partial \eta} \end{bmatrix}$$

$$[J2] = \begin{bmatrix} \left(\frac{\partial x}{\partial \xi}\right)^2 & \left(\frac{\partial y}{\partial \xi}\right)^2 & \frac{\partial x}{\partial \xi}\frac{\partial y}{\partial \xi} \\ \left(\frac{\partial x}{\partial \eta}\right)^2 & \left(\frac{\partial y}{\partial \eta}\right)^2 & \frac{\partial x}{\partial \eta}\frac{\partial y}{\partial \eta} \\ \frac{\partial x}{\partial \xi}\frac{\partial x}{\partial \eta} & \frac{\partial y}{\partial \xi}\frac{\partial y}{\partial \eta} & \frac{1}{2}\left(\frac{\partial x}{\partial \xi}\frac{\partial y}{\partial \eta} + \frac{\partial x}{\partial \eta}\frac{\partial y}{\partial \xi}\right) \end{bmatrix}$$

6. FORMULATION OF THE GEOMETRIC NON-LINEARITY

The geometrically nonlinear formulation [18] is done using [N]-notation formulated in [19] and the displacements referred to the original configuration following the Lagrangian method.

6.1 Equilibrium equation

The equilibrium equation is obtained by application of virtual principle as

$$\{\Psi\} = \int_V [B]^T \{\sigma\} dV - \{P\} = \{0\} \tag{17}$$

where $\{\psi\}$ denotes the sum of external and internal generalized forces and $[B]$ is obtained from the following relationship.

$$d\{\varepsilon\} = [B]\, d\{\delta\} \tag{18}$$

Again matrix $[B]$ may be expressed as

$$[B] = [B]_L + [B]_{NL} \tag{19}$$

where $[B]_L$ is the linear part and $[B]_{NL}$ is the nonlinear part and is dependent on displacements. If the strains are reasonably small, we can still write the elastic relationship

$$\{\sigma\} = \{D\}\{\varepsilon\} \tag{20}$$

Referring Eq.(8),

$$\{\varepsilon^p\}_{NL} = \frac{1}{2}\begin{bmatrix} \dfrac{\partial w}{\partial x} & 0 \\ 0 & \dfrac{\partial w}{\partial y} \\ \dfrac{\partial w}{\partial y} & \dfrac{\partial w}{\partial x} \end{bmatrix}\begin{Bmatrix} \dfrac{\partial w}{\partial x} \\ \dfrac{\partial w}{\partial y} \end{Bmatrix} = \frac{1}{2}[A]\{\theta\} \tag{21}$$

$$\{\theta\} = \begin{Bmatrix} \dfrac{\partial w}{\partial x} \\ \dfrac{\partial w}{\partial y} \end{Bmatrix} = \begin{Bmatrix} \dfrac{\partial}{\partial x}[N^b] \\ \dfrac{\partial}{\partial y}[N^b] \end{Bmatrix}\{\delta\} = [G]\{\delta\} \tag{22}$$

$$\{\varepsilon^p\}_{NL} = \frac{1}{2}[A][G]\{\delta\} = \frac{1}{2}[B^p]_{NL}\{\delta\} \tag{23}$$

$$\{\varepsilon\} = \left([B]_L + \frac{1}{2}[B]_{NL}\right)\{\delta\} \tag{24}$$

Referring Eqs.(21) and (24), Eq.(18) becomes

$$d\{\varepsilon\} = \{[B]_L\, d\{\delta\}\} + \{\frac{1}{2}\, d[A]\{\theta\} + \frac{1}{2}[A]\, d\{\theta\}\} \tag{25}$$

$$= \{[B]_L + [B]_{NL}\}\, d\{\delta\} \tag{26}$$

as, $d[A]\{\theta\} = [A]\, d\{\theta\} = [A][G]\, d\{\delta\} = [B]_{NL}\, d\{\delta\}$

With the help of Eqs.(19)-(24), Eq.(17) becomes

$$[K_S]\{\delta\} - \{P\} = \{0\} \tag{27}$$

where $[K_S]$ is the secant stiffness matrix and is given by

$$[K_S] = \int_V ([B]_L + [B]_{NL})^T [D]\left([B]_L + \frac{1}{2}[B]_{NL}\right) dV \tag{28}$$

$$[K_S] = \int_V [B]_L^T [D][B]_L \, dV + \frac{1}{2}\int_V [B]_L^T [D][B]_{NL} \, dV + \int_V [B]_{NL}^T [D][B]_L \, dV + \frac{1}{2}\int_V [B]_{NL}^T [D][B]_{NL} \, dV \tag{26}$$

$$= [K]_L + [K_S]_{NL} \tag{30}$$

where,

$[K]_L$ = Linear part of the stiffness matrix
$= \int_V [B]_L^T [D][B]_L \, dV$

$[K_S]_{NL}$ = Nonlinear part of the secant stiffness matrix
$= \frac{1}{2}\int_V [B]_L^T [D][B]_{NL} \, dV + \int_V [B]_{NL}^T [D][B]_L \, dV + \frac{1}{2}\int_V [B]_{NL}^T [D][B]_{NL} \, dV$

6.2 Incremental equilibrium equation

The tangent stiffness matrix is obtained by taking appropriate variation of Eq.(17) with respect to $\{\delta\}$,

$$\begin{aligned} d\{\psi\} &= \int_V d[B]^T \{\sigma\} dV + \int_V [B]^T \, d\{\sigma\} dV - d\{P\} \\ &= [K_T] \, d\{\delta\} - d\{P\} = \{0\} \end{aligned} \tag{31}$$

Substituting Eq.(19), (24) and (26) into Eq.(31), it yields to

$$\int_V d\left([B]_L + [B]_{NL}\right)^T \{\sigma\} dV + \int_V ([B]_L + [B]_{NL})^T [D]\left([B]_L + [B]_{NL}\right) dV \, d\{\delta\} - d\{P\} = \{0\} \tag{32}$$

$$[K_\sigma] d\{\delta\} + \left([K]_L + [K_T]_{NL}\right) d\{\delta\} = d\{P\} \tag{33}$$

$$[K_T] = [K]_L + [K_T]_{NL} + [K_\sigma] \tag{34}$$

$$[K_\sigma] d\{\delta\} = \int_V d[B]_{NL}^T \{\sigma\} dV \tag{35}$$

where,

$[K]_L$ = Linear part of the stiffness matrix $= \int_V [B]_L^T [D][B]_L \, dV$

$[K_T]_{NL}$ = Nonlinear part of the tangent stiffness matrix

$= \int_V \left([B]_L^T [D][B]_{NL} + [B]_{NL}[D][B]_L + [B]_{NL}^T [D][B]_{NL} \right) dV$

$[K_\sigma]$ = Initial stress matrix or Geometric stiffness matrix

6.3 Large deflection analysis in N-notation

Referring Eq.(23),

$$\left[B^p\right]_{NL} = [A][G] \tag{36}$$

$$[B]_{NL} = \begin{bmatrix} \left[B^p\right]_{NL} \\ \\ \left[B^b\right]_{NL} \end{bmatrix} = \begin{bmatrix} [A][G] \\ \\ [0] \end{bmatrix} \tag{37}$$

The volume integral is replaced by area integral, as the contribution across the thickness direction is considered in the rigidity matrix.

Using Eq.(6) and (36), Eq.(35) becomes

$$[K_\sigma] d\{\delta\} = \int_V d[B]_{NL}^T \{\sigma\} dV \tag{38}$$

$$= \int_A [G]^T \begin{bmatrix} d\dfrac{\partial w}{\partial x} & 0 & d\dfrac{\partial w}{\partial y} \\ \\ 0 & d\dfrac{\partial w}{\partial y} & d\dfrac{\partial w}{\partial x} \end{bmatrix} \begin{Bmatrix} N_x \\ N_y \\ N_{xy} \end{Bmatrix} dA \tag{39}$$

$$[K_\sigma] d\{\delta\} = \int_A [G]^T \begin{Bmatrix} d\dfrac{\partial w}{\partial x} N_x + d\dfrac{\partial w}{\partial y} N_{xy} \\ \\ d\dfrac{\partial w}{\partial y} N_y + d\dfrac{\partial w}{\partial x} N_{xy} \end{Bmatrix} dA \tag{40}$$

$$= \int_A [G]^T \begin{bmatrix} N_x & N_{xy} \\ N_{xy} & N_y \end{bmatrix} d \begin{Bmatrix} \dfrac{\partial w}{\partial x} \\ \\ \dfrac{\partial w}{\partial y} \end{Bmatrix} dA \tag{41}$$

$$= \int_A [G]^T [S]\, d\{\theta\} dA \tag{42}$$

$$= \int_A [G]^T [S][G]\, d\{\delta\} dA \tag{43}$$

$$[K_\sigma] = \int_A [G]^T [S][G] dA \tag{44}$$

where, $[S] = \begin{bmatrix} N_x & N_{xy} \\ N_{xy} & N_y \end{bmatrix}$

The secant stiffness matrix $[K_S]$ derived in Section-6.1 is unsymmetric in B-notation. In this context, N-notation [20] is used which gives symmetric secant stiffness matrix and is expressed as

$$[K_S] = [N_0] + \frac{1}{2}[N_1] + \frac{1}{3}[N_2]$$

$$[N_0] = \int_A [B]_L^T [D][B]_L \, dA$$

$$[N_1] = \int_A \left([B]_L^T [D][B]_{NL} + [B]_{NL}^T [D][B]_L + [G]^T [S]_L [G] \right) dA$$

$$[N_2] = \int_A \left([B]_{NL}^T [D][B]_{NL} + [G]^T [S]_{NL} [G] \right) dA$$

where, $[S]_L$ and $[S]_{NL}$ are the linear and nonlinear parts of the initial stress matrix.

7. NEWTON-RAPHSON METHOD

The nonlinear equations can be expressed as

$$\Psi\{\delta\} = [K_S\{\delta\}]\{\delta\} - \{P\} = \{0\} \tag{45}$$

Ignoring higher order terms, the function $\Psi\{\delta\}$ is expressed in terms of Taylor series as,

$$\Psi\left(\{\delta\}^{n+1}\right) = \Psi\left(\{\delta\}^n\right) + \left(\frac{d\{\Psi\}}{d\{\delta\}}\right)_n \{\Delta\delta\}^n = 0 \tag{46}$$

$$\text{where, } \{\delta\}^{n+1} = \{\delta\}^n + \{\Delta\delta\}^n \tag{47}$$

$$\{\Delta\delta\}^{n+1} = \left([K_T]^n\right)^{-1} \left(\{P\} - [K_S]^n \{\delta\}^n\right) \tag{48}$$

where,

$\{P\}$ = Load Level; $\{\Delta\delta\}^n$ = Incremental Displacement; $[K_T] = \dfrac{d\{\Psi\}}{d\{\delta\}}$

8. BOUNDARY CONDITIONS

As a general case, the stiffness matrix for a curved boundary supported on elastic springs continuously spread along the boundary line is used. Considering a local axis system $x_1 - y_1$ at a point P on a curved boundary along the direction of the normal to the boundary at that point as shown in the Fig.4, the displacement components along it can be obtained. Let β be the angle made by the local axis $x_1 - y_1$ with the global axis $x - y$ in the anticlockwise direction. Hence the relationship between the two axes is given by

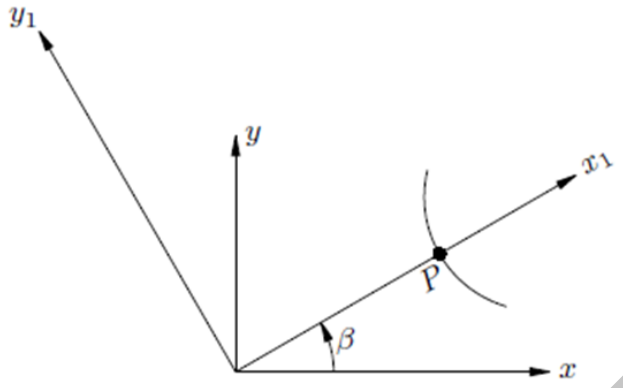

Figure 4. Co-ordinate axes at any point of an elastically restrained curved boundary

$$\begin{Bmatrix} x \\ y \end{Bmatrix} = \begin{bmatrix} \cos\beta & -\sin\beta \\ \sin\beta & \cos\beta \end{bmatrix} \begin{Bmatrix} x_1 \\ y_1 \end{Bmatrix} \tag{49}$$

The displacements at P which may be restrained can be expressed as

$$\{f_b\} = \begin{Bmatrix} u_1 \\ v_1 \\ w \\ \dfrac{\partial w}{\partial x_1} \\ \dfrac{\partial w}{\partial y_1} \end{Bmatrix} = \begin{bmatrix} \cos\beta & \sin\beta & 0 & 0 & 0 \\ -\sin\beta & \cos\beta & 0 & 0 & 0 \\ 0 & 0 & 1 & 0 & 0 \\ 0 & 0 & 0 & \cos\beta & \sin\beta \\ 0 & 0 & 0 & -\sin\beta & \cos\beta \end{bmatrix} \begin{Bmatrix} u \\ v \\ w \\ \dfrac{\partial w}{\partial x} \\ \dfrac{\partial w}{\partial y} \end{Bmatrix} \tag{50}$$

Expressing the above equation in terms of the shape function,

$$\{f_b\} = [N_b]\{\delta\} \tag{51}$$

where

$$[N_b] = \begin{bmatrix} \cos\beta & \sin\beta & 0 & 0 & 0 \\ -\sin\beta & \cos\beta & 0 & 0 & 0 \\ 0 & 0 & 1 & 0 & 0 \\ 0 & 0 & 0 & \cos\beta & \sin\beta \\ 0 & 0 & 0 & -\sin\beta & \cos\beta \end{bmatrix} \begin{Bmatrix} [N_u] \\ [N_v] \\ [N_w] \\ \dfrac{\partial [N_w]}{\partial x} \\ \dfrac{\partial [N_w]}{\partial y} \end{Bmatrix} \tag{52}$$

Let k_u, k_v, k_w, k_α and k_β be the spring constants or restraint coefficients corresponding to the direction of u, v, w, θ_n and θ_t respectively. The reaction components per unit length along the boundary line due to the spring constants corresponding to the possible boundary displacements are given by

$$\{f_k\} = \begin{Bmatrix} k_u u_1 \\ k_v v_1 \\ k_w w \\ k_\alpha \dfrac{\partial w}{\partial x_1} \\ k_\beta \dfrac{\partial w}{\partial y_1} \end{Bmatrix} \tag{535}$$

$$\{f_k\} = [N_k]\{\delta\} \tag{54}$$

where

$$[N_k] = \begin{bmatrix} k_u \cos\beta & k_u \sin\beta & 0 & 0 & 0 \\ -k_v \sin\beta & k_v \cos\beta & 0 & 0 & 0 \\ 0 & 0 & k_w & 0 & 0 \\ 0 & 0 & 0 & k_\alpha \cos\beta & k_\alpha \sin\beta \\ 0 & 0 & 0 & -k_\beta \sin\beta & k_\beta \cos\beta \end{bmatrix} \begin{Bmatrix} [N_u] \\ [N_v] \\ [N_w] \\ \dfrac{\partial [N_w]}{\partial x} \\ \dfrac{\partial [N_w]}{\partial y} \end{Bmatrix} \tag{55}$$

Using Eqs.(51) and (54), the stiffness matrix can be obtained by the virtual work principle and is expressed as

$$[K_b] = \int [N_b]^T [N_k] |J_b| d\lambda_1 \tag{56}$$

where λ_1 is the direction of the boundary line in the $\xi - \eta$ plane and J_b = Jacobian $= ds_1/d\lambda_1$. The jacobian is the ratio of actual length to the length of mapped domain at any segment of boundary length.

9. LOAD VECTOR

The consistent load vector [9] can be calculated from the principle of virtual work.

$$\{P\} = \int [N_w]^T q |J| d\xi d\eta \tag{57}$$

where q is the intensity of load acting on the plate.

Table 1: Different parameters used

Central deflection	w
Thickness	h
Uniformly distributed load	q
Concentrated load	p
Extreme fiber stress	$\sigma(x, y)$

10. RESULTS AND DISCUSSION

The proposed formulation is validated through a number of numerical examples. In each of the examples, the iteration process is continued until the total residual norm is within the prescribed tolerance limit as expressed by

$$\left((\Delta P^T \Delta P)/(P^T P)\right)^{0.5} \times 100 \le \gamma \tag{58}$$

where γ is the tolerance for the convergence and it is taken as 0.1%. The analyses for plate of different planforms such as square, skewed, circular, elliptical, annular, trapezoidal, semicircular, right angled triangular, equilateral triangular, semi-circular semi-elliptical, diamond and axe-head shaped are carried out with mesh divisions for the whole plate. The deflections and stresses obtained at critical points are compared with the published and SAP 2000 results wherever possible. Also, some examples of clamped square, rectangular, skew and circular plate under uniformly distributed load by the same authors using the present method can be found in [21]. The different parameters used are tabulated in Table 1 and the non-dimensional form for loads, deflections and stresses are given in Table 2. The boundary conditions applied are

$u = v = w = \theta_x = \theta_y = 0$, for clamped edge and

$u = v = w = 0$, for simply supported edge.

10.1 Rectangular plate

Square plate in Fig.5 with two edges simply supported and other two free is analyzed and compared in Table 3. Different aspect ratios (1.0, 1.5 and 2.0) are considered for all the edges simply supported boundary conditions and the results for 32×32 mesh division are shown in Table 4-5.

Table 2: Non-dimensional form

Central deflection	W	w/h
Uniformly distributed load	Q	$(qa^4)/Eh^4$
Concentrated load	P	$(pa^2)/Eh^4$
Extreme fiber stress	$\sigma'(x,y)$	$(\sigma(x,y)a^2)/(Eh^2)$

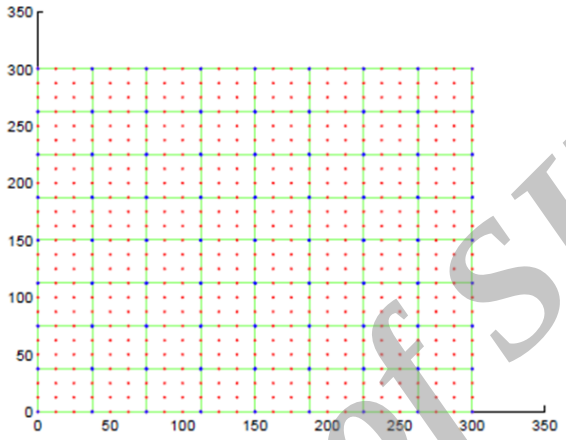

$a = 300cm$; $h = 3.0cm$; $\nu = 0.316$; $E = 0.3\times10^8\ N/cm^2$

Figure 5. A typical 8×8 mesh discretization with boundary nodes of square plate

Table 3: Square plate with the two edges simply supported and the other two free

Load (N/cm)	Central Deflection W			Moment $(N\text{-}cm)$		Inplane Force (N)	
q	Milasinovic [22]	Present	SAP	Present	SAP	Present	SAP
1.0	0.3318	0.3449	0.3449	881.2693	882.2648	943.8344	943.7994
2.5	0.5537	0.5780	0.5779	1460.9	1461.818	2664.8	2664.5150
5.0	0.7686	0.7954	0.7951	1983.6	1983.69	5079.4	5077.273
7.5	0.9179	0.9422	0.9420	2326.3	2325.883	7162.2	7160.504
10.0	1.0352	1.0569	1.0567	2588.2	2585.902	9045.3	9043.573

Table 4: Deflection $W = w/h$ at the center of the simply supported rectangular plate

Load Factor	b/a = 1.0	b/a = 1.5	b/a = 2.0
17.79	0.5450	0.7533	0.8104
38.3	0.8281	1.0592	1.1081
63.4	1.0416	1.2902	1.3365
95	1.2309	1.4976	1.5442
134	1.4102	1.6966	1.7454
184	1.5826	1.8902	1.9424
245	1.7547	2.0853	2.1419
318	1.9239	2.2786	2.3400
402	2.0871	2.4663	2.5327

Table 5: Stress $\sigma' = \sigma a^2/Eh^2$ at the center of the simply supported rectangular plate

Load Factor	b/a = 1.0	b/a = 1.5	b/a = 2.0
17.79	4.3881	5.8130	6.1066
38.3	7.1796	8.9021	9.1177
63.4	9.5160	11.5466	11.7503
95	11.7789	14.1736	14.4051
134	14.1106	16.9354	17.2225
184	16.5418	19.8560	20.2192
245	19.1660	23.0388	23.4963
318	21.9443	26.4296	26.9949
402	24.8184	29.9505	30.6322

10.2 Skew plate

The deflection and central stress of simply supported skewed plate shown in Fig.6 are compared with published results in Fig.7-8 respectively.

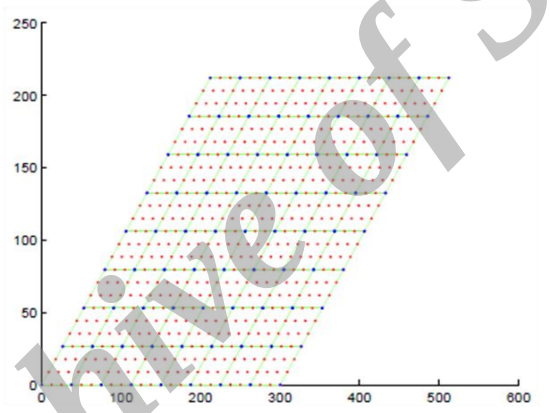

$a = 300cm$; $h = 3.0cm$; $\nu = 0.316$; $E = 0.3\times10^8\, N/cm^2$

Figure 6. A typical 8×8 mesh discretization with boundary nodes of skew plate

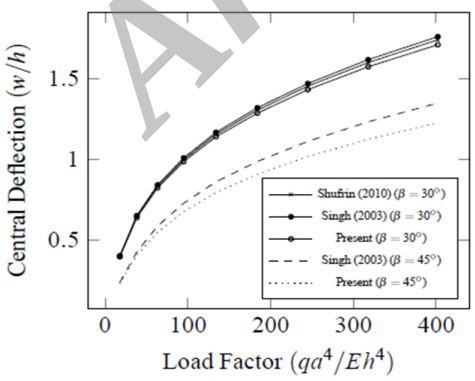

Figure 7. Central deflection of simply supported skew plate

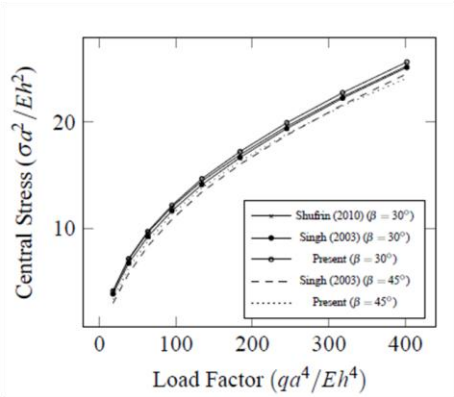

Figure 8. Central stress of simply supported skew plate

10.3 Circular plate

A circular plate shown in Fig. 9 is analyzed and results for clamped case are compared with published ones for concentrated load in Fig. 10-11. The present results for simply supported circular plate under uniformly distributed load (udl) and point load are given in Table 6 for 24×24 mesh division.

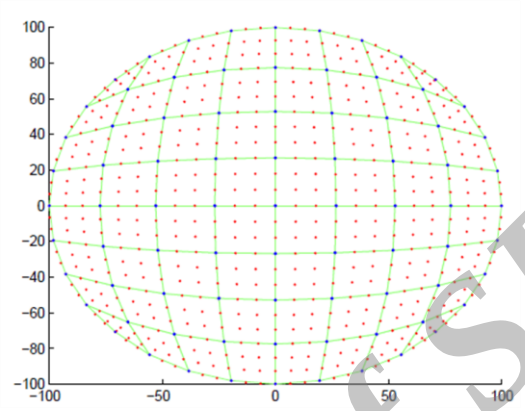

$r=100cm;\ h=2.0cm;\ \nu=0.3;E=0.1\times10^{8}\ N/cm^{2}$

Figure 9. A typical 8×8 mesh discretization with boundary nodes of circular plate

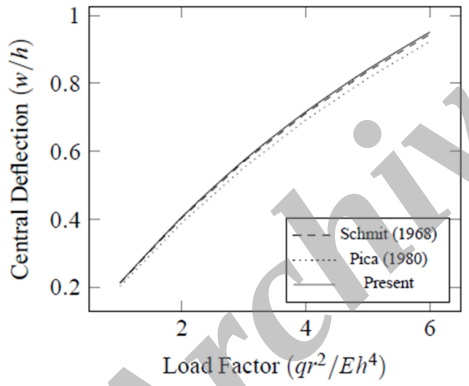

Figure 10. Central deflection of clamped circular plate under concentrated load

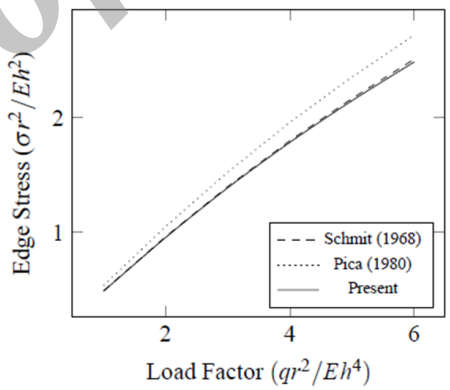

Figure 11. Edge stress of clamped circular plate under concentrated load

Table 6: Central deflection and stress in simply supported circular plate

under udl			under point load		
Load Factor	Central Deflection	Central Stress	Load Factor	Central Deflection	Central Stress
1	0.4795	1.0348	1	0.4365	2.3556
2	0.7035	1.6261	2	0.6863	4.3564
3	0.8517	2.053	3	0.8631	6.1561
6	1.1385	2.9678	4	1.004	7.8342
10	1.3826	3.8515	5	1.1232	9.426
15	1.6008	4.7342	6	1.2275	10.951

10.4 Elliptical plate

Table 7 presents the results with 24×24 mesh size for both clamped and simple supports of elliptic plate shown in Fig.12 under uniformly distributed load where a and b are taken as semi-minor and semi-major axes of the plate respectively.

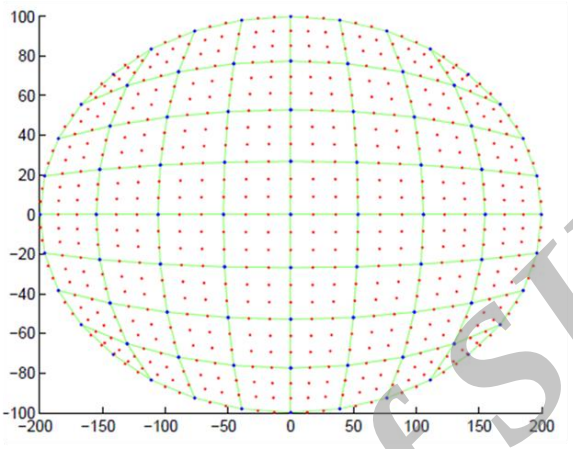

$a = 100cm; b = 200cm;\ h = 2.0cm;\ \nu = 0.3;\ E = 0.1\times10^8\ N/cm^2$

Figure 12. A typical 8×8 mesh discretization with boundary nodes of elliptical plate

Table 7: Deflection and stress in elliptical plate under uniformly distributed load

Boundaries	Clamped						Simply Supported	
Load Factor	Central Deflection		Central Stress		Mid-edge Stress		Central Deflection	Central Stress
	Weil [23]	Present	Weil [23]	Present	Weil [23]	Present	Present	Present
1	0.344	0.3505	0.862	0.9	1.705	1.6023	0.7303	1.3994
2	0.600	0.614	1.550	1.6486	3.322	3.0375	0.9858	2.0384
3	0.789	0.8086	2.077	2.2268	4.76	4.2827	1.1546	2.5069
6	1.163	1.1945	3.217	3.429	8.289	7.3441	1.4869	3.5477
10	1.490	1.5205	4.333	4.519	11.970	10.6358	1.777	4.593
15	1.790	1.8088	5.490	5.5656	15.656	14.1227	2.0441	5.6611

10.5 Annular plate

An annular plate (Fig.13) of sector angle ($\theta = 60°$) is analyzed under uniformly distributed load and the deflection, membrane forces and bending moments at center are compared for clamped boundary conditions in Fig.14 -16. r_o and r_i are outer and inner radius of the plate respectively. The results for the case of simply supported boundary condition are given in Table 8 for 24×24 mesh division.

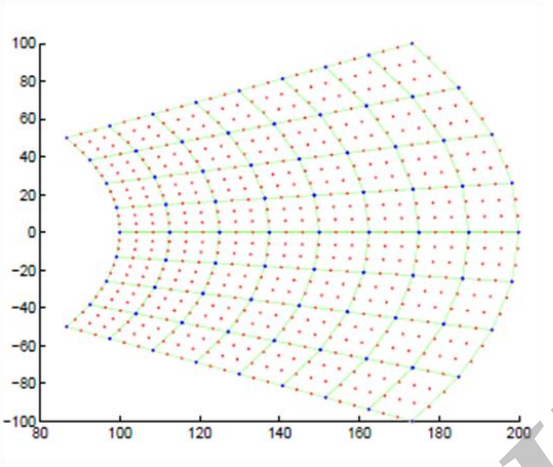

$\frac{r_i}{r_o} = 0.5\ ;\ a = r_o - r_i\ ;\ h = 2.0cm;\ \nu = 0.3;\ E = 0.1\times10^8\ N/cm^2$

Figure 13. A typical 8×8 mesh discretization with boundary nodes of annular plate

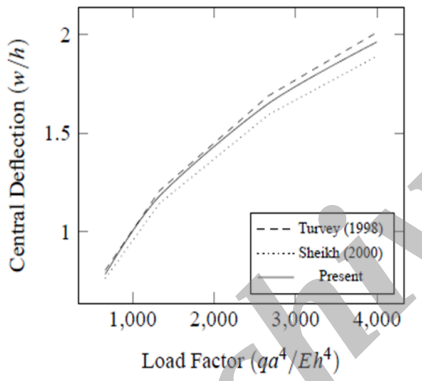

Figure 14. Central deflection of clamped annular plate

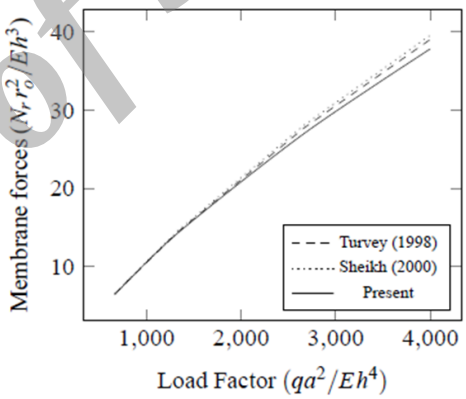

Figure 15. Membrane forces at center of clamped annular plate

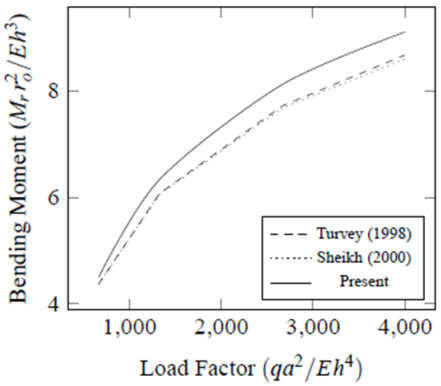

Figure 16. Bending moments at center of clamped annular plate

Table 8: Central deflection and forces in simply supported annular plate

Load Factor	Central Deflection w/h	Membrane Force $N_r r_o^2/(Eh^3)$	$N_\theta r_o^2/(Eh^3)$	Bending Moment $M_r r_o^2/(Eh^4)$	$M_\theta r_o^2/(Eh^4)$
666.7	1.1496	13.7285	8.121	4.0567	1.8795
1333.3	1.4986	23.2935	14.143	5.0545	2.1249
2666.7	1.9163	38.2685	23.753	6.1317	2.3816
4000	2.2013	50.82	31.832	6.8112	2.5557

10.6 Trapezoidal plate

In Table 9, results are presented for central deflection and stress for a clamped and simply supported trapezoidal plate (Fig. 17) for 24×24 mesh division. α and β are the angles made by left and right edge of trapezoid to X -axis. $L_x =$ base length of trapezoid and $L_y =$ slant length of left edge of trapezoid.

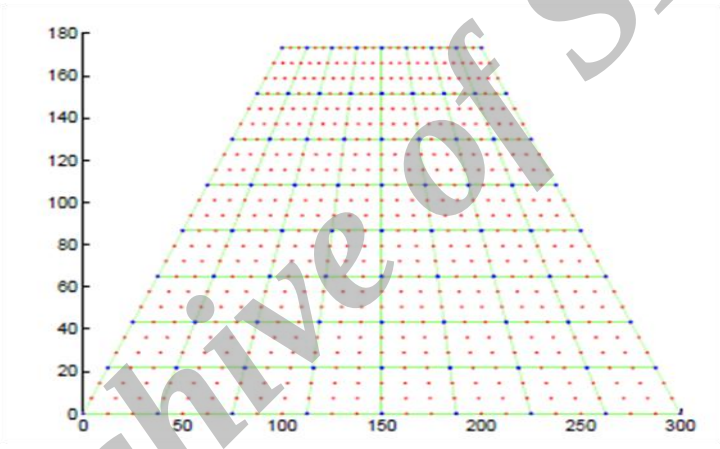

$\alpha = 60\,;\ \beta = 120\,;\ \frac{L_x}{L_y} = 1.5\,;\ \nu = 0.3; E = 0.1\times10^8\ N/cm^2$

Figure 17. A typical 8×8 mesh discretization with boundary nodes of trapezoidal plate

Table 9. Deflection and stress in trapezoidal plate

Boundaries	Clamped					Simply Supported	
Load Factor	Central Deflection		Central Stress		Mid-edge Stress	Central Deflection	Central Stress
	Shufrin [24]	Present	Shufrin [24]	Present	Present	Present	Present
5	0.0422	0.0429	0.578	0.5872	1.2493	0.142	1.3134
10	0.0842	0.0855	1.168	1.1875	2.5023	0.2652	2.5713
50	0.3908	0.3961	5.834	5.9146	12.2128	0.7686	8.7014
100	0.678	0.686	10.589	10.7238	22.7819	1.0555	12.8863
200	1.0521	1.064	17.124	17.337	39.8275	1.3894	18.4819

10.7 Semicircular Plate

A semicircular plate (Fig. 18) is analyzed for a clamped and simply supported boundary conditions and the results for 24×24 mesh division are shown in Table 10 and 11 respectively. The deflection and stress at coordinate $(0, 56.66)$ and mid stress at bottom edge are calculated. $r =$ radius of the semicircle.

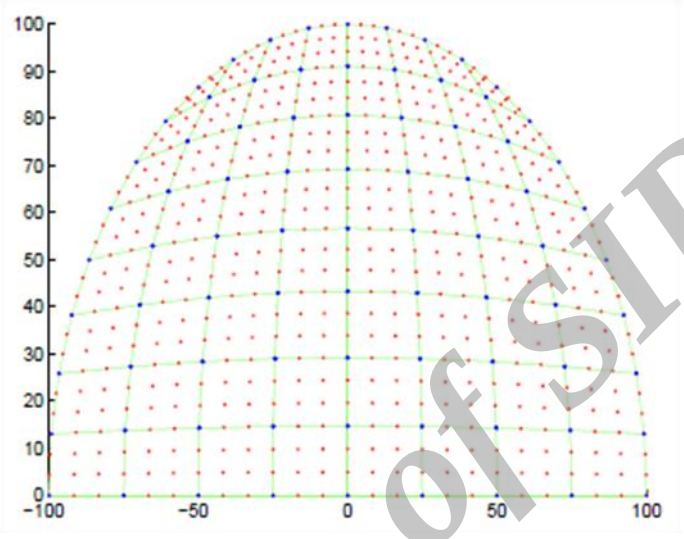

$r = 100cm;\ h = 2.0cm;\ \nu = 0.3;\ E = 0.1\times 10^8\ N/cm^2$

Figure 18. A typical 8×8 mesh discretization with boundary nodes of semicircular plate

Table 10: Deflection and stress in clamped semicircular Plate

Load Factor	Deflection		Stress		Mid-edge Stress	
	Present	SAP	Present	SAP	Present	SAP
25	0.467	0.470	4.977	5.024	10.136	8.667
50	0.773	0.781	8.719	8.782	18.367	16.010
75	0.988	0.999	11.496	11.554	25.189	21.328
100	1.154	1.169	13.733	13.770	31.155	25.735
125	1.292	1.309	15.638	15.645	36.549	29.560

Table 11: Deflection and stress in simply supported semicircular plate

Load Factor	Deflection		Stress	
	Present	SAP	Present	SAP
25	0.855	0.829	7.046	6.839
50	1.134	1.109	10.173	9.920
75	1.322	1.297	12.518	12.214
100	1.468	1.443	14.490	14.132
125	1.590	1.565	16.241	15.824

10.8 Right-angled Triangular Plate

The deflection and stress at coordinate $(37.5, 37.5)$ and $(56.25, 37.5)$ for b/a =1.0 and 1.5 respectively and mid stress at bottom edge of right angled plate (Fig. 19) are presented for clamped and simply supported boundary conditions in Table 12-15 for 24×24 mesh division.

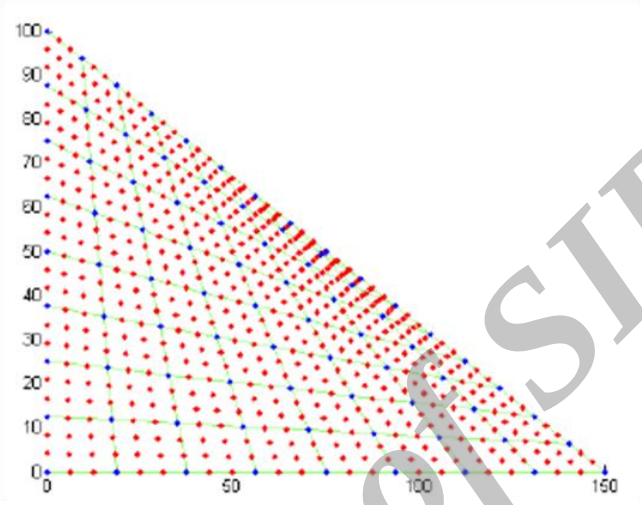

$a = 100cm$; $h = 2.0cm$; $\nu = 0.3$; $E = 0.1\times10^8\ N/cm^2$

Figure19. A typical 8×8 mesh discretization with boundary nodes of right-angled triangular plate

Table 12: Deflection and stress in clamped right-angled triangular plate for $b/a = 1$

Load Factor	Central Deflection		Central Stress		Mid-edge Stress	
	Present	SAP	Present	SAP	Present	SAP
300	0.411	0.418	11.583	11.229	27.132	25.607
350	0.464	0.471	13.339	12.878	31.268	29.588
400	0.514	0.521	15.015	14.440	35.282	33.471
450	0.560	0.568	16.615	15.922	39.180	37.261
500	0.630	0.611	18.143	17.331	42.969	40.965

Table 13: Deflection and stress in simply supported right-angled triangular plate for $b/a = 1$

Load Factor	Deflection		Stress	
	Present	SAP	Present	SAP
300	0.794	0.783	18.884	17.541
350	0.849	0.838	20.595	19.125
400	0.898	0.888	22.180	20.586
450	0.943	0.932	23.665	21.949
500	0.985	0.973	25.068	23.233

Table 14: Deflection and stress in clamped right-angled triangular plate for $b/a = 1.5$

Load Factor	Deflection		Stress		Mid-edge Stress	
	Present	SAP	Present	SAP	Present	SAP
300	0.640	0.648	17.464	17.031	36.962	38.016
350	0.707	0.716	19.607	19.075	41.866	43.386
400	0.768	0.777	21.605	20.969	46.528	48.347
450	0.824	0.833	23.480	22.739	50.981	53.221
500	0.876	0.885	25.253	24.402	55.251	57.932

Table 15: Deflection and stress in simply supported right-angled triangular plate for $b/a = 1.5$

Load Factor	Deflection		Stress	
	Present	SAP	Present	SAP
300	1.008	1.010	22.712	21.645
350	1.071	1.073	24.652	23.481
400	1.127	1.129	26.460	25.176
450	1.179	1.181	28.163	26.771
500	1.227	1.228	29.780	28.290

10.9 Equilateral Triangular Plate

The results of equilateral triangular Plate (Fig. 20) are shown for a clamped and simply supported boundary conditions in Table 16 and 17 respectively for 24×24 mesh size. The deflection and stress at coordinate $(56.25, 32.475)$ and mid stress at bottom edge are presented.

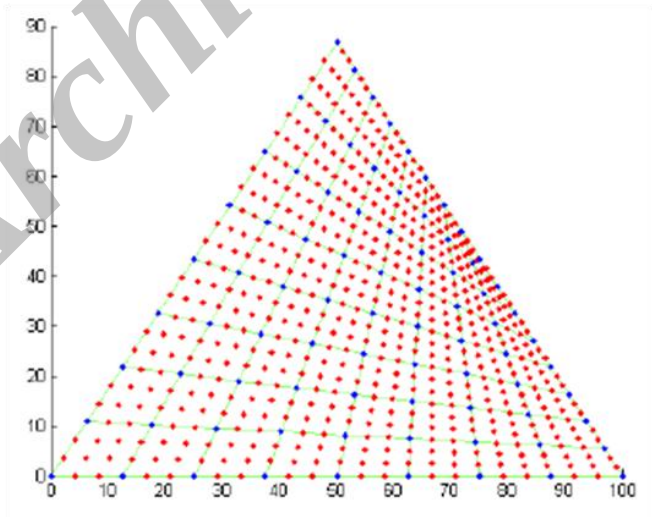

$a = 100cm$; $h = 2.0cm$; $\nu = 0.3$; $E = 0.1\times10^{8}\, N/cm^{2}$

Figure 20. A typical 8×8 mesh discretization with boundary nodes of equilateral triangular plate

Table 16: Deflection and stress in clamped equilateral triangular plate

Load Factor	Deflection		Stress		Mid-edge Stress	
	Present	SAP	Present	SAP	Present	SAP
300	0.436	0.453	14.041	14.173	32.847	37.055
350	0.495	0.513	16.123	16.247	37.754	42.665
400	0.549	0.569	18.097	18.209	42.487	48.063
450	0.600	0.621	19.970	20.066	47.056	53.291
500	0.648	0.669	21.747	21.825	51.474	58.352

Table 17: Deflection and stress in simply supported equilateral triangular plate

Load Factor	Deflection		Stress	
	Present	SAP	Present	SAP
300	0.840	0.819	20.525	20.021
350	0.900	0.879	22.340	21.873
400	0.953	0.933	24.009	23.574
450	1.002	0.982	25.564	25.156
500	1.046	1.027	27.025	26.641

10.10 Semi-circular Semi-elliptical Plate

A plate (Fig. 21) consisting of a semicircle and semi-ellipse is analyzed. In Table 18, results for central deflection and stresses in a clamped and simply supported boundary conditions are shown for 16×16 mesh division. Here, r = radius of the semicircle, a and b are semi-minor and semi-major axis of the plate.

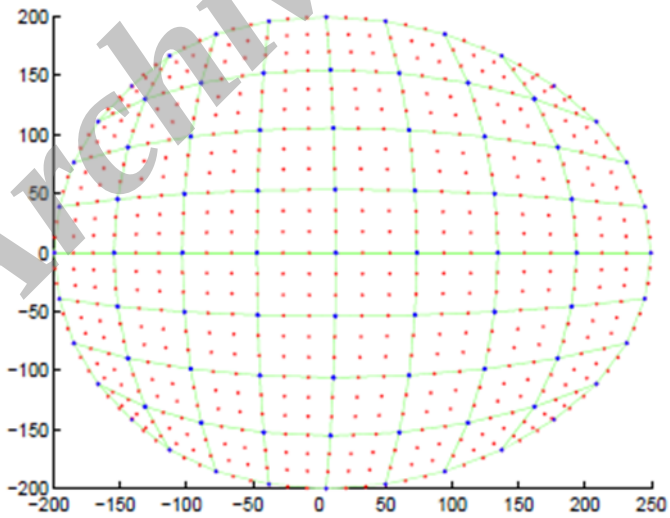

$a = r = 200cm;\ b = 250cm;\ h = 2.0cm;\ \nu = 0.3\ ;E = 0.1\times10^{8}\ N/cm^{2}$

Figure 21. A typical 8×8 mesh discretization with boundary nodes of semi-circular semi-elliptical plate

Table 18: Central deflection and stress in semi-circular semi-elliptical plate

Boundaries	Clamped			Simply Supported	
Load	Central Deflection	Central Stress	Mid-edge Stress	Central Deflection	Central Stress
1	0.2056	0.5919	0.8767	0.5435	1.1386
2	0.3888	1.1653	1.7287	0.7784	1.7512
3	0.5437	1.6737	2.5245	0.9333	2.1941
6	0.8832	2.8378	4.5955	1.2339	3.1504
10	1.1818	3.9084	6.8788	1.4909	4.082
15	1.4451	4.8997	9.3054	1.7215	5.0172

10.11 Diamond Shaped Plate

A diamond shaped plate (Fig. 22 and Fig. 23) are analyzed for $r2/r1=1.0$ and 1.5 respectively. In Table 19 and 20, results for central deflection and stresses in a clamped and simply supported boundary conditions are shown for 32×32 mesh division. Here, $r1, r2$ = radii of the arcs.

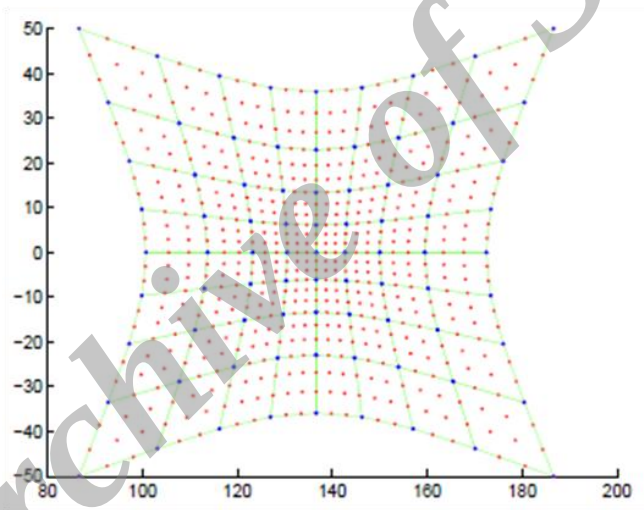

$r2/r1=1.0$; $r1=100cm$; $h=2.0cm$; $\nu=0.3$; $E=0.1\times10^8\ N/cm^2$

Figure 22. A typical 8×8 mesh discretization with boundary nodes of diamond shaped plate for $r2/r1=1.0$

Table 19: Central deflection and stress in diamond shaped plate for $r2/r1=1.0$

Boundaries	Clamped			Simply Supported	
Load	Central Deflection	Central Stress	Mid-edge Stress	Central Deflection	Central Stress
300	0.8676	18.6576	45.1430	1.1941	20.3071
350	0.9546	20.6878	51.1530	1.2709	22.0355
400	1.0329	22.5304	56.8642	1.3397	23.6182
450	1.1042	24.2230	62.3197	1.4021	25.0997
500	1.1696	25.7914	67.5537	1.4595	26.4988

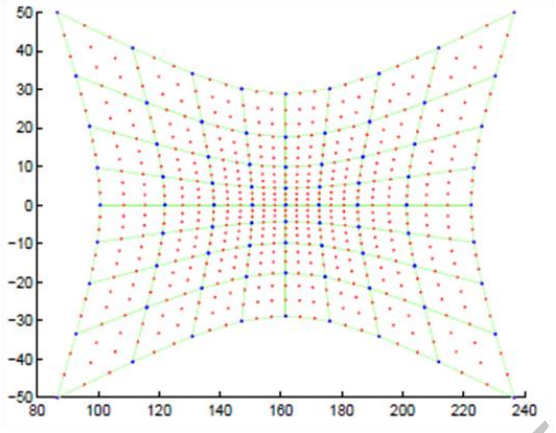

$r2/r1 = 1.5;\ r1 = 100cm;\ h = 2.0cm;\ \nu = 0.3\ ;\ E = 0.1\times10^{8}\ N/cm^{2}$

Figure 23. A typical 8×8 mesh discretization with boundary nodes of diamond shaped plate for $r2/r1 = 1.5$

Table 20: Central deflection and stress in diamond shaped plate for $r2/r1 = 1.5$

Boundaries	Clamped			Simply Supported	
Load	Central Deflection	Central Stress	Mid-edge Stress	Central Deflection	Central Stress
300	0.7733	22.3848	51.1662	1.1114	25.2125
350	0.8493	24.8401	57.7238	1.1780	27.2463
400	0.9177	27.0040	63.9263	1.2380	29.1343
450	0.9799	29.0333	69.8305	1.2927	30.9060
500	1.0371	30.9201	75.4810	1.3432	32.5822

10.12 Axe-head Shaped Plate

An axe-head shaped plate (Fig.24) is analyzed and results for central deflection and stresses in a clamped and simply supported boundary condition for 32×32 mesh size are shown in Table 21. Here, r = radius of the arc.

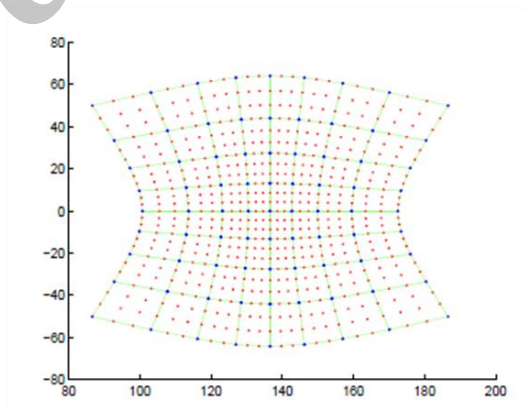

$r2/r1 = 1.0;\ r1 = 100cm\ ;\ h = 2.0cm;\ \nu = 0.3\ ;\ E = 0.1\times10^{8}\ N/cm^{2}$

Figure 24. A typical 8×8 mesh discretization with boundary nodes of axe-head shaped plate

Table 21: Central deflection and stress in axe-head shaped plate

Boundaries	Clamped			Simply Supported	
Load	Central Deflection	Central Stress	Mid-edge Stress	Central Deflection	Central Stress
50	0.3805	6.7852	7.6882	0.7326	9.7435
100	0.6580	12.1953	14.6086	0.9996	14.2688
150	0.8593	16.2654	20.7650	1.1749	17.5599
200	1.0161	19.5075	26.3491	1.3100	20.2857
250	1.1450	22.2296	31.4986	1.4220	22.6767

11. CONCLUSIONS

The formulation for large deflection of thin plates of arbitrary shape is generalized by means of a mapping technique so that the analysis is performed in a square domain. Many researchers have used different elements to analyze plates but these elements are limited to solve a particular type of geometry only. The isoparametric element though elegant in its formulation to accommodate different geometries but is deficient with regard to its behavior because of the presence of shear locking and spurious mechanisms and cannot be fully alleviated even if with reduced and selective integration. In the present investigation,the element has all the advantages of the isoparametric element to model an arbitrary plate shape and without the disadvantages of the shear locking problem etc. The versatility of the element is proved by undertaking different plate geometries such as square, rectangle, skew, circle, ellipse, annular, and trapezoidal. Also, semicircular, right angled triangle, equilateral triangle shaped geometries along with some complex geometries are analyzed and compared with SAP 2000. In this context, the formulation is done in the total Lagrangian co-ordinate system and Newton-Raphson technique is used to solve nonlinear governing equations.The results obtained for various geometries of the plate are validated with the available ones which are found to be in excellent agreement.

REFERENCES

1. Levy S. Square plate with clamped edges under normal pressure producing largdeflections, NASA Technical Note 847.
2. Bogner FK, Fox RL, Schmidt LA. The generation of inter-element compatible stiffness and mass matrices by the use of interpolation formulae, *Proceedings of the Conference on Matrix Methods in Structural Analysis*, Wright-Patterson A.F.B., 1965.
3. Schmit R. Large deflections of a clamped circular plate, *Journal of the Engineering Mechanics Division, ASCE*, No. EM6, **94**(1968) 1603-6.
4. Rushton KR. Large deflection of plates with initial curvature, *International Journal of Mechanical Sciences*, **12**(1970) 1037-51.
5. Pica A, Wood RD, Hinton E. Finite element analysis of geometrically nonlinear plate behavior using a Mindlin formulation, *Computers and Structures*, No. 3, **11**(1980) 203-15.

6. Cheung YK, Dashan Z. Large deflection analysis of arbitrary shaped thin plates, *Computers and Structures*, No. 5, **26**(1987) 811-4.
7. Turvey GJ, Salehi M. Elastic large deflection analysis of stiffened annular sector plates, *International Journal of Mechanical Sciences*, No. 1, **40**(1998) 51-70.
8. Singh AV, Elaghabash Y. On the finite displacement analysis of quadrangular plates, *International Journal of Non-Linear Mechanics*, **38**(2003) 1149-62.
9. Sheikh AH, Mukhopadhyay M. Geometric nonlinear analysis of stiffened plates by the spline finite strip method, *Computers and Structures*, **76**(2000) 765-85.
10. Shahidi AR, Mahzoon M, Saadatpour MM, Azhari M. Nonlinear static analysis of arbitrary quadrilateral plates in very large deflections, *Communications in Nonlinear Science and Numerical Simulation*, **12**(2007) 832-48.
11. Das D, Sahoo P, Saha K. A variational analysis for large deflection of skew plates under uniformly distributed load through domain mapping technique, *International Journal of Engineering, Science and Technology*, No. 1, **1**(2010) 16-32.
12. Wankhade RL. Geometric nonlinear analysis of skew plates using finite element method, *International Journal of Advanced Engineering Technology*, No. II, **II**(2011) 154-63.
13. Adini A, Clough RW. Analysis of Plate Bending by the Finite Element Method, Report submitted to the National Science Foundation, G7337(1961).
14. Melosh RJ. Basis for derivation of matrices for the direct stiffness method, *AIAA Journal*, **1**(1963) 1631-7.
15. Barik M, Mukhopadhyay M. Finite element free flexural vibration analysis of arbitrary plates, *Finite Elements in Analysis and Design*, **29**(1998) 137-51.
16. Zienkiewich OC, Taylor RL. *The Finite Element Method*, 4th ed, McGraw-Hill, 1989.
17. Barik M, Mukhopadhyay M. A new stiffened plate element for the analysis of arbitrary plates, *Thin-Walled Structures*, **40**(2002) 625-39.
18. Mukhopadhyay M, Sheikh AH. *Matrix and Finite Element Analyses of Structures*, Ane Books Pvt. Ltd, 2004.
19. Mallet R, Marcal P. Finite element analysis of nonlinear structures, *Journal of Structural Division, ASCE*, **94**(1968) 2081-2105.
20. Wood RD, Schrefler B. Geometrically nonlinear analysis - a correlation of finite element methods, *International Journal of Numerical Methods in Engineering*, **12**(1978) 635-42.
21. Panda S, Barik M. Geometrically nonlinear finite element analysis of arbitrary thin plates, Implementing Innovative Ideas in Structural Engineering and Project Management, *Proceedings of ISEC-8, 2015*, pp. 469-74.
22. Milasinovic DD. Geometric non-linear analysis of thin plate structures using the harmonic coupled finite strip method, *Thin-Walled Structures*, **49**(2011) 280-90.
23. Weil NA, Newmark NM. Large deflections of elliptical plates, *Journal of Applied Mechanics, ASME*, No. 1, **23**(1956) 21-6.
24. Shufrin I, Rabinovitch O, Eisenberger M. A semi-analytical approach for the geometrically nonlinear analysis of trapezoidal plates, *International Journal of Mechanical Sciences*, No. 12, **52**(2010) 1588-96.